

A Thesis

On

**“Effect of Particle Size on the Compressive
Strength of Cement”**

Submitted in Partial fulfilment of the requirement for the award of the degree of

Master of Technology (M.Tech.)

IN

MATERIALS SCIENCE AND ENGINEERING

Submitted By

CHETAN SHARMA
ROLL No.:60602005

Under the able guidance of

Dr. KULVIR SINGH
Assistant Professor
School of Physics and Material Sciences
Thapar University, Patiala



**SCHOOL OF PHYSICS AND MATERIAL SCIENCE
THAPAR UNIVERSITY, PATIALA
PATIALA (PUNJAB) -147001, INDIA**

June 2008

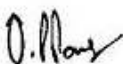
*Dedicated to my Loving Grand
Parents*


CERTIFICATE

*This is to certify that the thesis entitled “Effect of particle size on the compressive strength of cement” submitted by Mr. Chetan Sharma Roll No. 60602005 in partial fulfillment of the requirement for the award of the degree of **MASTERS OF TECHNOLOGY** in **Materials Science and Engineering**, Thapar University Patiala, is a record of candidates own work carried out by him under our supervision and guidance. The matter embodied in this report is of the candidate’s own record and not submitted to any other university in any part or full form for the award of such kind of a degree.*


(Dr. KULVIR SINGH)
Supervisor
SPMS, Thapar University
Patiala

Countersigned by:


Dr. O. P. Pandey
(Prof. & Head)
School of Physics and Materials Science
Thapar University, Patiala


Dr. R. K. Sharma
Dean of Academic Affairs
Thapar University, Patiala

ACKNOWLEDGEMENT

Knowledge in itself is a continuous process. I would have never succeeded in completing my task without the cooperation, encouragement and help provided to me by various personalities. With deep sense of gratitude I wish to express my sincere thanks to **Dr. Kulvir Singh** Assistant Professor School of Physics and Materials Science, who have been constant sources of inspiration for me throughout this project work.

I express my sincere thanks to my esteemed and worthy supervisor, **Dr. O.P.Panday**, Professor and head, School of Physics and Materials Science, for his valuable guidance in caring out this work under his effective supervision, encouragement and unforgettable cooperation.

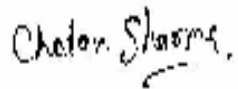
I would like to thank all the teaching staff for their full motivation and appreciation to my work. My thanks to P G Lab in charge Mr. Purushottam. His assistance and partnership were of great pleasure.

I would also like to give many thanks to Research Scholars Mr. Vishal Chaudhary, Mr. Ravi Shukla, Mr. Akshay kumar and Mr. Sanjeev Kumar for any kind of help and valuable suggestions whenever I needed out of their busy schedule. All my friends and my colleagues at the Materials Science & Engineering program and the School of Physics and Material Sciences are acknowledged for providing me a friendly atmosphere and encouraging me throughout this work.

Beside all these I am grateful to the whole quality control team of Ambuja Cement Limited, **Mr. S. S. Sodhi HR (GM)** and **Mr. A. K. Rastogi (GM Quality Control)** my guide who gave me the all necessary and valuable suggestion for completion of project. Special thanks to Mr. C. L. Shukla (Physical lab of ACL), Mr. Raju Ram Sharma (Physical lab of ACL), Mr. Vinod Sharma (XRF Analyser), Mr. Mohan Lal Sharma (Particle size analyser), Mr. Ramesh Thakur, Mr. Mohan Srivastva, Mr. Surender Verma, Mr. Lekh Raj, Mr. Aggarwal, Mr. Harish Sharma who helps me during the whole project. Beside all, thanks to the management of ACL Darlaghat distt. Solan (H.P) who gave me opportunity to work in their plant. With out whose blessing this project can never be completed.

Special thanks to Mr.Amar Singh and Mr. Inder pal gauger in the physical lab who helps me in making the samples of concrete because there are 14 blocks has been made every day for measuring the compressive strength.

I am deeply thankful to my Family, their moral support and patience has born fruit through completion of this Thesis which will result in award of the prestigious degree of M.Tech Materials science & Engineering.

A handwritten signature in black ink that reads "Chetan Sharma". The signature is written in a cursive style with a small flourish at the end.

Chetan Sharma

Roll No.60602005

Abstract

Cement is very essential part of the modern life. In the present study, the effects of the particle size and their distribution on mechanical and structural properties are explained via few experimental studies. The seven samples of cement were selected for the study. These samples were grind unit ball mill for different time duration. Their mean particle size is reduced substantially by ball milling. The ball milled samples were characterized viz x-ray diffraction, particle size analyser and x-ray fluorescence. These samples of cement are mixed with standard sand in a definite proportion for the manufacturing of blocks. Then their compressive strength is measured by compressive strength machine. It is observed that lower particle size exhibit higher compressive strength with lower setting time.

Contents	Page No.
Certificate	
Acknowledge	
Abstract	
Chapter -1	Introduction
1.1 Background	6
1.2 Portland cement	6
1.3 Various Types of Cements	7
1.3.1 Ordinary Portland cement	7
1.3.2 Portland Pozzalana Cement	7
1.3.3 Portland Blast Furnace Slag Cement	7
1.3.4 Oil Well Cement	7
1.3.5 Rapid Hardening Cement	7
1.3.6 Sulphate Resisting Portland Cement	7
1.3.7 White Cement	7
1.3.8 Clinker Cement	7
1.4 Cement Manufacturing Process	7
1.4.1 Dry Process	8
1.4.2 Semi Dry Process	9
1.4.3 Semi Wet Process	10
1.4.4 Wet Process	11

1.5	Setting and Hardening	12
Chapter -2 Literature Review		
2	Literature Review	17
Chapter -3 Experimental Detail		
3.1	Sample Preparation	21
3.2	X-Ray Fluorescence Analysis	21
3.3	XRD technique	22
3.4	Blaine Apparatus	23
3.4.1	Working of Blaine Apparatus	24
3.4.2	Specification of the instrument	24
3.5	Particle size Analyser	24
3.5.1	Measurement Technique	24
3.5.2	Experimental	25
3.5.3	Measuring Particle size by Using Laser Diffraction	25
3.5.4	Measurement Using Two Laser Diffraction Particle Size analysers	26
3.6	Ball Milling	26
3.6.1	Grinding Media	27
3.7	Compressive Strength Machine	28
Chapter-4 Result and Discussion		
4.1	X-Ray Fluorescence	30
4.2	Important Factors and Chemical Analysis	30
4.2.1	Lime Saturation Factor	30
4.2.2	Silica Ratio	31

4.2.3	Alumina Ratio	31
4.3	Clinker: The Bogue Ratio	31
4.4	Particle Size Analysis	32
4.5	XRD	36
4.6	Compressive Strength Measurements	37

Chapter -5 Conclusion & Future Scope

References

List of Tables and Figures.

Tables:

Table 1. The compressive strength and hardening time

Table 2. Specifications of Blaine Apparatus

Table 3. Chemical composition of the sample determined by XRF

Table 4. Surface area with mean diameter and milling time of different samples

Table 5. Variation of compressive strength of samples with days

Diagrams:

Figure 1. Production of cement by dry process

Figure 2. Production of cement by semi wet process

Figure 3. Production of cement by wet process

Figure 4. Schematic arrangement of wave length dispersive spectrometer

Figure 5. Geometric arrangement of XRD

- Figure 6. Blaine fineness Apparatus
- Figure 7. Particle size analyser
- Figure 8. Grinding media with cement powder
- Figure 9. Compressive strength machine
- Figure 10. Particle diameter (μm) with respect to volume percentage of sample PPC1
- Figure 11. Particle diameter (μm) with respect to volume percentage of sample PPC2
- Figure 12. Particle diameter (μm) with respect to volume percentage of sample PPC3
- Figure 13. Particle diameter (μm) with respect to volume percentage of sample PPC4
- Figure 14. Particle diameter (μm) with respect to volume percentage of sample PPC5
- Figure 15. Particle diameter (μm) with respect to volume percentage of sample PPC6
- Figure 16. Particle diameter (μm) with respect to volume percentage of sample PPC7
- Figure 17. XRD pattern of samples (a) PPC3 (b) PPC5 (c) PPC7
- Figure 18. Graph between compressive strength and mean particle size
- Figure 19. Graph between compressive strength and days

CHAPTER-1

INTRODUCTION

1.1 Background

Portland cement was developed from hydraulic limes in the early part of the nineteenth century in Britain. Its name is derived from the Portland stone, a type of building stone that was quarried on the Isle of Portland in Dorset, England. Joseph Aspdin was received a patent in 1824 on process technique to make the cement which is called Portland cement. William in 1843 made an improved version of Portland cement and he initially called it "Patent Portland cement". In 1848 William Aspdin further improved the quality of cement. Many technologist and researcher have claimed to make the first Portland cement in the modern sense, but it is generally accepted that it was first manufactured by William Aspdin at Northfleet, England in 1842. The German Government issued a standard on Portland cement in 1878.

1.2 Portland Cement

Portland cement is the most common type of cement in general usage in many parts of the world. It is a fine powder produced by grinding Portland cement clinker (more than 90%), a limited amount of calcium sulfate which controls the set time, and up to 5% minor constituents. As defined by the European Standard EN197.1, "Portland cement clinker is a hydraulic material which shall consist of at least two-thirds by mass of calcium silicates ($3\text{CaO}\cdot\text{SiO}_2$ and $2\text{CaO}\cdot\text{SiO}_2$), the remainder consisting of aluminum- and iron-containing clinker phases and other compounds". The ratio of CaO to SiO_2 should not be less than 2.0. The magnesium content (MgO) should not be exceeded 5.0% by mass. A homogeneous mixture of raw materials is heated $1450\text{ }^\circ\text{C}$ to make the portland cements. The aluminum oxide and iron oxide are present as a flux and contribute little to the strength. For special cements, such as Low Heat (LH) and Sulfate Resistant (SR) types, it is necessary to limit the amount of tricalcium aluminate ($3\text{CaO}\cdot\text{Al}_2\text{O}_3$). The major raw material for the clinker-making[8] is usually improved limestone (CaCO_3). Which contains SiO_2 as an impurity. The CaCO_3 content of these limestones can be as high as 80%. Secondary raw materials (materials in the raw mix other than limestone) depend on the purity of the limestone. Some of the secondary raw materials used are: clay, shale, sand, iron

ore, bauxite, fly ash and slag. The ash of the coal acts as a secondary raw material when a cement kiln is fired by coal.

1.3 Various Types of Cement

The types of cement have increased over the years with the advancement in processing techniques. Various types of cement produced are as follows:

1.3.1 Ordinary Portland Cement

1.3.2 Portland Pozzolana Cement

1.3.3 Portland Blast Furnace Slag Cement

1.3.4 Oil Well Cement

1.3.5 Rapid Hardening Portland Cement

1.3.6 Sulphate Resisting Portland Cement

1.3.7 White Cement

1.3.8 Clinker Cement

1.4 Cement Manufacturing Process

Historically, the development of the cement manufacturing processes are categorized in four process[15] routes namely dry, wet, semi wet and semi dry processes. Apart of these techniques dry process is most economical and advanced technique. Their advantages and disadvantages are summarized in the following section.

1.4.1 Dry Process

In this process, the raw material is grinding and drying in tube mills or vertical roller mills, in presence of hot kiln exhaust gases or cooler exhaust air for drying. Prior to being fed to the kiln, the raw meal is homogenized or blended either in batch type or in continuously operating homogenizing silo systems. Dry process production unit is given in figure 1.

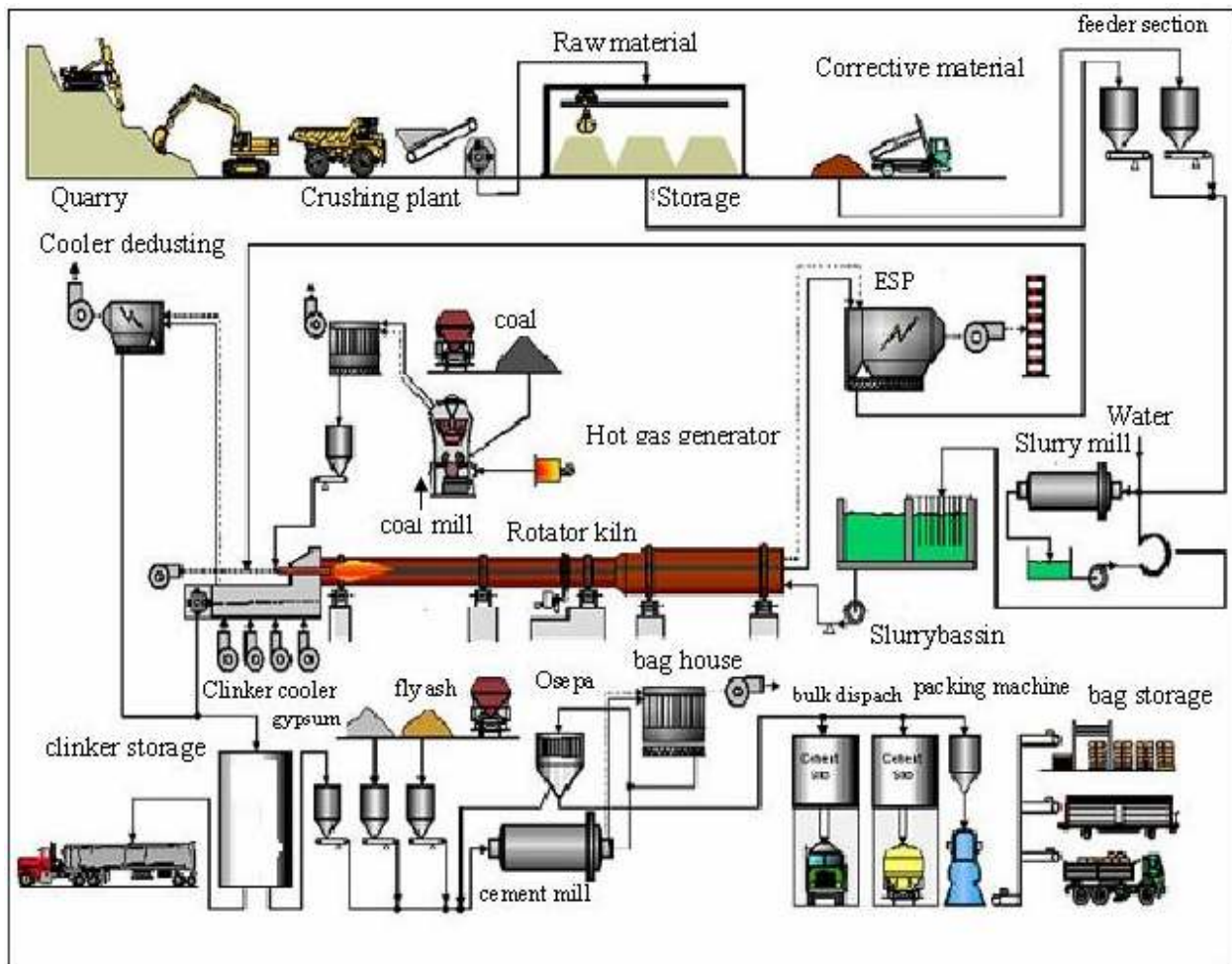


Figure 1 Production of cement by dry process

In suspension preheater kilns, the raw mill is fed to the top of a series of cyclones passing down in stepwise counter-current flow with hot exhaust gases from the rotary kiln thus providing

intimate contact and efficient heat exchange between solid particles and hot gas. The cyclones thereby serve as separators between solids and gas. Prior to entering the rotary kiln, the raw meal is calcined at 810-830°C. The exhaust gases leave the preheater at a temperature of 300-360 °C and are further utilised for raw material drying in the raw mill. Six stage preheater kilns are susceptible to blockages and build-ups caused by excessive input of elements such as sulfur, chlorides or alkalis which are easily volatilised in the kiln system. This input has to be carefully controlled. Excessive input may require the installation of a system which allows part of the rotary kiln gases to bypass the preheater. Thereby part of the volatile compounds are extracted together with the gas. A bypass system extracts a portion (typically 5-15 %) of the kiln gases from the riser pipe between the kiln and preheater. This gas has a high dust burden. It is cooled with air, volatile compounds are condensed onto the particulates and the gas then passes through a dust filter. Modern suspension preheater kilns usually have 4 cyclone stages with a maximum capacity limited to approximately 4000 ton /day. In some cases, 2- stage cyclone preheaters or 1-stage preheaters supported by internal chain heat exchangers are also used. A considerable capacity can be increase with precalciner kilns with a second combustion device between the rotary kiln and the preheater section. Kiln systems with five to six stage cyclone preheater and precalciner are considered standard technology for new plants today, as the extra cyclone stages improve thermal efficiency. In some cases, the raw mill is fed directly to a long dry kiln without external preheater. A system of chains in the inlet part of the rotary kiln provides the heat exchange between the hot combustion gases from the hot zone of the kiln and the kiln feed. Long dry kilns have high heat consumption and high dust cycles requiring separate dedusting cyclones.

1.4.2 Semi Dry Process

In the semi-dry process, dry raw meal is pelletised with 10-12 % of water on an inclined rotating table (granulating disc) and fed to a horizontal travelling grate preheater in front of the rotary kiln (Lepol system). The pelletised material is dried, pre-heated and partly calcined on the two-chamber travelling grate making use of the hot exhaust gases from the kiln. A higher degree of calcination can be achieved by burning part of the fuel in the hot chamber of the grate preheater. The hot exhaust gases from the kiln first pass through a layer of preheated pellets in the hot chamber. After intermediate dedusting in cyclones, the gases are drawn once again through a layer of moist pellets in the drying chamber of the grate. As much of the residual dust is

precipitated on the moist pellet bed, the total dust load of the exhaust gases at the preheater outlet is low.

As a drawback of the semi-dry process, kiln exhaust gases cannot be fully utilised in the raw mill drying and grinding system due to the low temperature level. The maintenance costs of grate preheaters are high. Modern installations rarely use the semi-dry process.

1.4.3 Semi Wet Process

The semi wet process is shown in figure 2. In this process the raw slurry is dewatered in filter presses. Typically, modern chamber filtration systems produce filter cakes with a residual moisture content of 16-21 %. In the past, filter cakes were further processed in extruders to form pellets which were then fed to grate preheater kilns with three chambers.

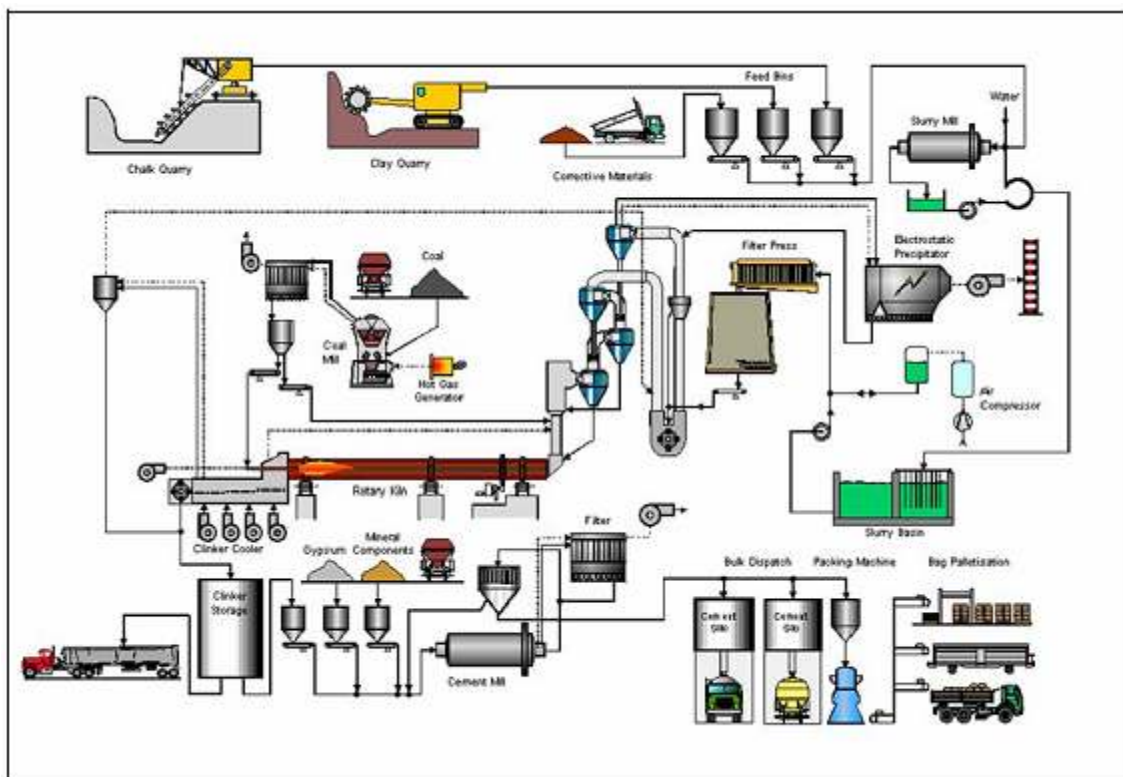


Figure 2 Production of cement by semi-wet process

In modern cement plants, slurry filtration is applied only where raw materials have a very high natural moisture content, i.e. chalk. Filter cake coming from the filter presses is kept in intermediate storage bins before it is fed to heated crushers or dryers where a dry raw meal is produced which is fed to a modern preheater or precalciner kiln. With the dryers/crushers operating full time in parallel with the kiln (compound operation), these systems have a very good energy recovery by making full use of the kiln exhaust gases and the cooler exhaust air.

1.4.4 Wet Process

Conventional wet process kilns are the oldest type of rotary kilns to produce clinker. Wet kiln feed (raw slurry) typically contains 28 to 43 % of water which is added to the raw mill (slurry drums, wash mills and/or tube mills). Batch blending and homogenization is achieved in special slurry silos or slurry basins where compressed air is introduced and the slurry is continuously stirred. The slurry is pumped into the rotary kiln where the water has to be evaporated in the drying zone at the kiln inlet. The drying zone is designed with chains and crosses to facilitate the heat exchange between the kiln feed and the combustion gases. After having passed the drying zone as shown in figure 3 the raw material moves down the kiln to be calcined and burnt to clinker in the sintering zone. Conventional wet kiln technology has high heat consumption and produces large volumes of combustion gases and water vapour.

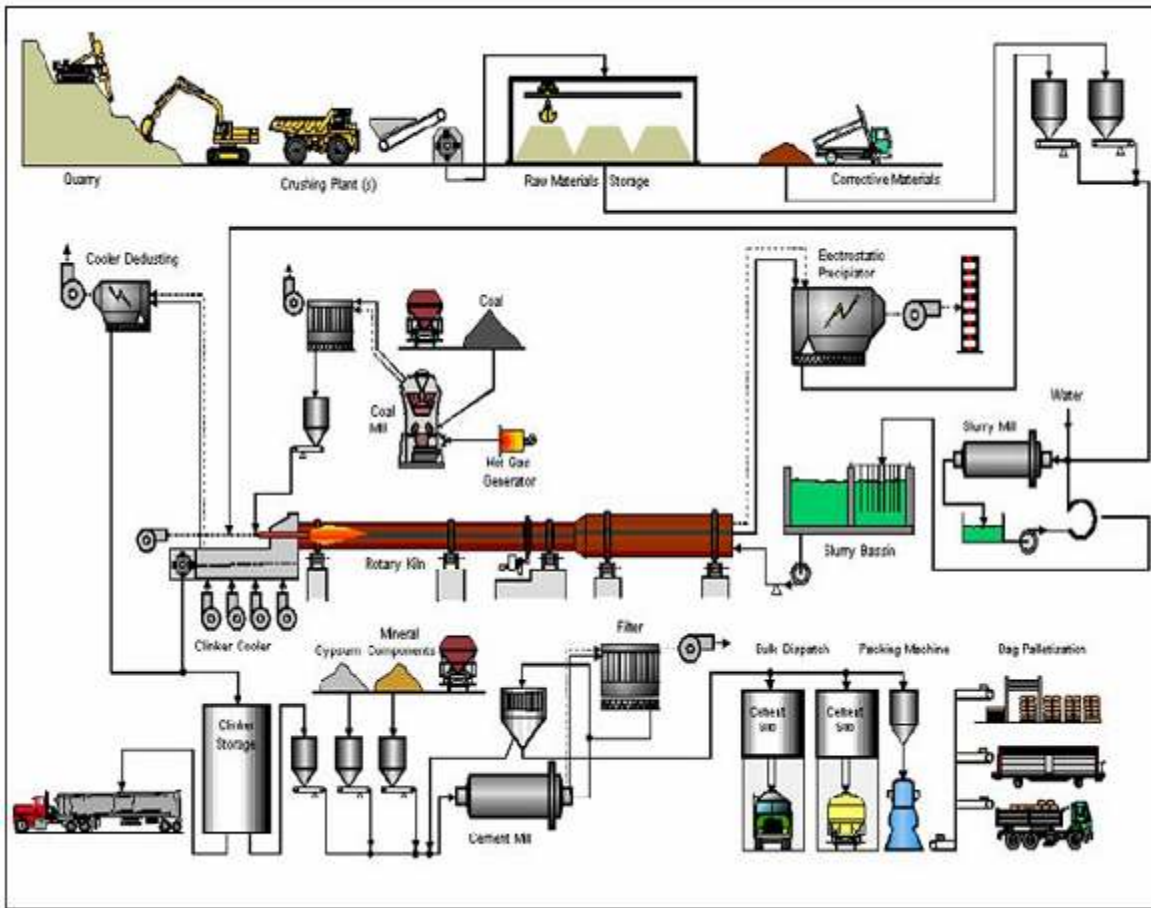


Figure 3 Production of cement by wet process

Wet rotary kilns may reach a total length of up to 240 m compared to short dry kilns (55 to 65 meter). In modern wet kiln systems, the raw slurry is fed to slurry drier where the water is evaporated prior to the dried raw meal entering a cyclone preheater/precalciner kiln. Modern wet kiln systems have a far lower specific heat consumption compared to conventional wet kilns.

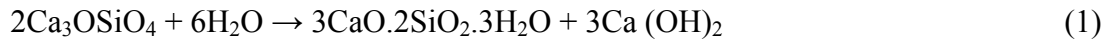
1.5 Setting and Hardening

When water is mixed with Portland cement, the product sets in a few hours and hardens over a period of weeks. These processes can vary widely depending upon the mix used and the conditions of curing of the product, but a typical concrete sets (i.e. becomes rigid) in about 6 hours, and develops a compressive strength. The compressive strength and hardening time period is given in the table 1.

Table 1 *The compressive strength and hardening time*

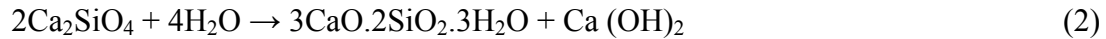
Hardening Time period (Hours)	Compressive Strength (MPa)
24	8
72	23
168	35
672	41

In principle, the strength continues to rise slowly as long as water is available for continued hydration, but concrete is usually allowed to dry out after a few weeks, and this causes strength growth to stop. Setting and hardening of Portland cement is caused by the formation of water-containing compounds, forming as a result of reactions between cement components and water. Usually, cement reacts in a plastic mixture only at water/cement ratios between 0.25 and 0.75. The reaction and the reaction products are referred to as hydration and hydrates or hydrate phases, respectively. As a result of the reactions a stiffening can be observed which is very small in the beginning, but which increases with time. The point in time at which it reaches a certain level is called the start of setting. The consecutive further consolidation is called setting, after which the phase of hardening begins. Stiffening, setting and hardening are caused by the formation of a microstructure of hydration products of varying rigidity which fills the water-filled interstitial spaces between the solid particles of the cement paste, mortar or concrete. The behavior with time of the stiffening, setting and hardening therefore depends to a very great extent on the size of the interstitial spaces, i.e. on the water/cement ratio. The hydration products primarily affecting the strength are calcium silicate hydrates (C-S-H phases). Further hydration products are calcium hydroxide, sulfatic hydrates (AFm and AFt phases), and related compounds, hydrogarnet, and gehlenite hydrate. Calcium silicates or silicate constituents make up over 70 % by mass of silicate-based cements. The hydration of these compounds and the properties of the calcium silicate hydrates produced are therefore particularly important. Calcium silicate hydrates contain less CaO than the calcium silicates in cement clinker, so calcium hydroxide is formed during the hydration of Portland cement. This is available for reaction with supplementary cementitious materials such as ground granulated blast furnace slag and pozzolana. The simplified reaction of alite with water may be expressed as:

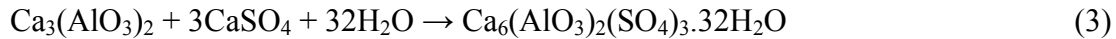


This is a relatively fast reaction, causing setting and strength development in the first few weeks.

The reaction of belite is



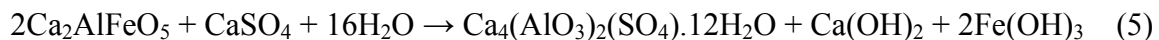
This reaction is relatively slow, and is mainly responsible for strength growth after one week. Tricalcium aluminate hydration [33] is controlled by the added calcium sulfate, which immediately goes into solution when water is added. Firstly, ettringite is rapidly formed, causing a slowing of the hydration (see tricalcium aluminate)



The ettringite subsequently reacts slowly with further tricalcium aluminate to form "monosulfate" - an "AFm phase"



This reaction is complete after 1-2 days. The calcium aluminoferrite reacts slowly due to precipitation of hydrated iron oxide



The pH-value of the pore solution reaches comparably high values and is of importance for most of the hydration reactions.

Soon after Portland cement is mixed with water, a brief and intense hydration starts (pre-induction period). Calcium sulfates dissolve completely and alkali sulfates almost completely. Short, hexagonal needle-like ettringite crystals form at the surface of the clinker particles as a result of the reactions between calcium- and sulphate ions with tricalcium aluminate. Further, originating from tricalcium silicate, first calcium silicate hydrates (C-S-H) in colloidal shape can be observed. Caused by the formation of a thin layer of hydration products on the clinker surface, this first hydration period ceases and the induction period starts during which almost no reaction

takes place. The first hydration products are too small to bridge the gap between the clinker particles and do not form a consolidated microstructure. Consequently the mobility of the cement particles in relation to one another is only slightly affected; i. e. the consistency of the cement paste turns only slightly thicker. Setting starts after approximately one to three hours, when first calcium silicate hydrates form on the surface of the clinker particles, which are very fine-grained in the beginning. After completion of the induction period, a further intense hydration of clinker phases takes place. This third period (accelerated period) starts after approximately four hours and ends after 12 to 24 hours. During this period a basic microstructure forms, consisting of C-S-H needles and C-S-H leafs, platy calcium hydroxide and ettringite crystals growing in longitudinal shape. Due to growing crystals, the gap between the cement particles is increasingly bridged. During further hydration, the hardening steadily increases, but with decreasing rate. The density of the microstructure rises and the pores fill. The filling of pores with respect of time and hydration increases the compressive strength of the cement.

CHAPTER-2

LITRATURE REVIEW

Particle size affects not only the strength but also has some effect on the heat of hydration, shrinkage, expansion. These factors ultimately affect the strength of cement. Therefore a lot of research are being carried out to reduce the cost and increases the strength of cement. This chapter deals with the review of the literature.

F. Skvra et al. [2] studied the technological properties of pastes and mortars with low water-to-cement ratio bicarbonate depend upon clinker particle size distribution. These properties cannot be described explicitly as a function of specific surface area. The granulometric composition of clinker particles according to idealised curves represent a specific optimum state to be reached at given water volume as well as maximum short term strength values.

P.Dale bentz[10] observed that the original size, spatial distribution, and composition of Portland cement particles have a large influence on hydration, microstructure development, and ultimate properties of cement-based materials. the effects of cement particle size distribution on a variety of performance properties are explored via computer simulation and a few experimental studies. Properties examined include setting time, heat release, capillary porosity percolation, diffusivity, chemical shrinkage, autogenous shrinkage and internal relative humidity evolution. The computer simulations are conducted using seven cement particle size distributions. Apart from these studies three different water-to-cement (w/c) ratios: i.e. 0.5, 0.3, and 0.246 are also reported. For lower w/c ratio systems, the use of coarser cements may offer equivalent or superior performance, as well as reducing production costs for the manufacturer.

Inclusion size affect was reported by central des ponts at chausses in light weight concrete. According to them the compressive strength of expanded polystyrene (EPS) lightweight concrete increases significantly with a decrease in EPS bead size for the same concrete (macro) porosity (p).To confirm that the scaling phenomenon is an intrinsic particle size effect and is related to the EPS bead size .A compressive tests have been carried out on homothetic EPS concrete specimens containing homothetic EPS beads. Moreover, five concrete (macro) porosities ranging from 10% to 50% have also been investigated. Compressive tests results have confirmed the

presence of a particle size effect on the EPS concrete compressive strength. Further more, it is observed that the size effect is very pronounced for low porosity concretes and becomes negligible for very high porosity concretes. The study was conducted on various samples. The result shows the similarity with experimental result.

Hanifi Binici et al. [16] examined the effect of particle size distribution on the properties of blended cements incorporating ground granulated blast furnace slag (GGBFS) and natural pozzolan (NP). Pure Portland cement (PPC), NP and GGBFS were used to obtain blended cements that contain 10, 20, 30% additives. The cements were produced by intergrinding and separate grinding and then blending. Each group had two different Blaine fineness of 280 m²/g and 480 m²/g. According to the particle size distribution (PSD) curves, 46% of the coarser specimens and 69% of the finer specimens passed through the 20 µm sieve. It was observed that the separately ground specimens were relatively finer than the interground ones and had higher compressive strength and sulfate resistance. The separately ground coarser specimens had the lowest heat of hydration. The separately ground finer specimens, which had the highest compressive strength and sulfate resistance, had the highest percent passing for each sieve size. For these specimens 34, 69, 81 and 99% passed through 5, 20, 30 and 55 µm sieves, respectively. For the interground specimens, which had the same fineness, the respective values for the same sieves were 32, 68, 75 and 94%. Compressive strength and density of no-fines concrete mixture dependent on the processing and degree of compaction. The role of cement content in bonding the coarse aggregate and in controlling the strength and density of no-fines concrete is illustrated. The optimum water-cement ratio for different compaction methods was determined.

M.P. Ginebra et al [19] examined in this work the possibility of controlling the final micro structural features of calcium phosphate cement by modifying the particle size of the starting powder, and to study the effect of this parameter on the kinetics of the setting reaction. The development of calcium phosphate materials with tailored structures at the micro and nanoscale levels could allow the modulation of some specific responses in biological phenomena such as protein adsorption and cell adhesion, which strongly depend on the nano-sized roughness of the interface. It is shown that the higher specific surface, produced by the reduction of the particle size of the powder, strongly accelerates the hydrolysis of the α -TCP into calcium-deficient

hydroxyapatite. The higher degree of super saturation attained in the solution favours the nucleation of smaller crystals. Thus, by increasing the specific surface area of the starting powder in a factor of 5, the size of the precipitated crystals is strongly reduced, and the specific surface of the set cement increases by a factor of 2. The reduction of the particle size produces a substantial decrease of the setting time and accelerates the hardening of the cement without significantly affecting the final strength attained. The mechanical strength achieved by the cement cannot be univocally related to the degree of reaction, without considering the micro structural features.

N Moayed et al [21] studied the effect of particle size of aggregate and low water cement ratio on paste falling quantity, void content, flow value, and compressive strength and bending strength which are physical properties of porous concrete. They concluded that increases in voids decreases the compressive strength of the sample. Smaller particle size exhibit higher compressive strength.

Ginebra et al [19] showed that the small aggregate is a necessary ingredient in concrete. In Oklahoma there are several different types of sands that can be used. Various types of sand were mixed with concrete and study the effect on the compressive strength of the concrete. This test was repeated after 3 days, 7 days, and 28 days. The sands were then screened to determine the particle size of each sand. Based on the data collected for this project, the following conclusion has been drawn: the sand in the concrete influence the strength of concrete. However variation in the in the particle size of sand could not show appropriable effect on the strength.

P.K.Panigraphy et al [15] studied the relationship between the particle size distribution (PSD) and their physical properties. It was found that the cement grind in different mills showed variation in the strength. Particles between 5 to 10 μm sizes show almost linear relationship with strength.

K.L.un et al [55] reported the effect of the addition of nano SiO_2 on sludge ash-cement mortar. The addition of nano- SiO_2 can shorter the setting time of the cement. Additionally the sludge ash of greater fineness can improve the compressive strength of the mortar. The nano- SiO_2 additive is also beneficial for the compressive strength of the mortar with different ash particle.

CHAPTER-3

EXPERIMENTAL DETAILS

3.1 Sample Preparation

The cement is taken with normal size with blaine value $3931\text{cm}^2/\text{gm}$. The size of cement dust is then reduced with the help of ball milling to the $5065\text{cm}^2/\text{gm}$. They are then separately collected in the different jars. Then with the help of X-ray fluorescence the chemical composition of cement samples are calculated. After determined the chemical composition the particle size in volume percentage is determined with the help of particle size analyser, which can calculate the particle size of 1 micron in volume percentage. There are the graphs between particle size and volume percentage which show the volume percentage of cement particle in different size. Now the cement is ready for the preparation of sample. All the preparations of sample are done in the Physical laboratory. The ratio of cement with sand is taken 1:3. The sand is taken the standard quality. There are three different type of sand is taken. These are taken 200gm of each sand. These samples are prepared by mixing a suitable quantity of water to cement ratio by calculating the normal consistency. Then sample is prepared by mixing the water, sand and cement of different blaine. After preparing the sample they are put in the humidity chamber for the one day. Then these samples are put in the water tank for different time duration. After completion of desired days these blocks of concretes are put under the compressive strength machine for measuring the compressive strength. This is calculated in KN. This is the brief technique how sample is prepared and strength is noted. But beside these, there are also some chemical analysis are done by (XRF) for chemical composition, (XRD) for Phases, Particle size and Blaine for fineness.

3.2 X-Ray Fluorescence Analysis

XRF is a very versatile instrument to analyse the chemical composition of given sample. It is non destructive technique. In principle, the lightest element that can be analysed is beryllium ($Z = 4$), but due to instrumental limitations and low x-ray yields from the light elements, it is often difficult to quantify elements lighter than sodium ($Z = 11$), unless background corrections and

very comprehensive inter element corrections are made. The mechanism of XRF are given in figure 4.

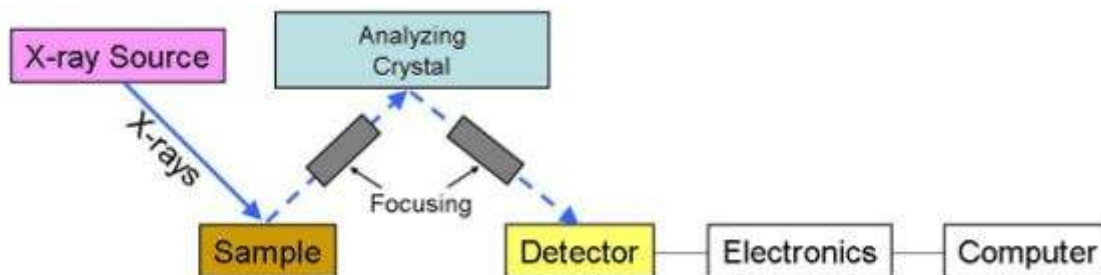


Figure 4 Schematic arrangement of wavelength dispersive spectrometer

3.3 X-Ray Diffraction Technique

X-ray diffraction analysis (XRD) is a non-destructive, very versatile technique to determine the crystalline phases and their volume fractions. The sample is irradiated with monochromatic X-rays and the reflected radiation is recorded by the counters. In this technique various forms of the samples could be used and very less amount is required for phase determination. The X-ray diffraction patterns were recorded using Rigaku model Geiger diffractogram with CuK α radiation ($\lambda = 1.5418\text{\AA}$) obtained from copper target using an in built Ni filter. The 2θ values for XRD patterns were generally taken in the range of 5° to 100° for most of the samples at a scan speed of $5^\circ/\text{min}$. The inter planar spacing (d) values of samples were calculated using the Bragg's law.

$$2d \sin \theta = n \lambda \quad (6)$$

Where λ is the wavelength of incident X-ray, d is the interplanar distance and θ is diffraction angle. The XRD patterns were identified using Powder Diffraction files (PDF). The geometric representation of Bragg's law is given in figure 5.

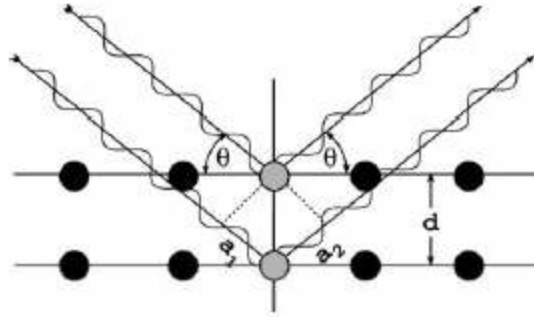


Figure 5 Geometric representation of x-ray diffraction

Geometric derivation of Bragg's law: constructive interference occurs when the delay between the waves scattered from adjacent lattice planes given by $a_1 + a_2$ is an integer multiple of the wavelength λ .

3.4 Blaine Apparatus

Blaine apparatus is used to measure the surface area of the particles. The blaine apparatus is shown in figure 6.



Figure 6 Blaine Fineness Apparatus

3.4.1 Working of Blaine Apparatus

It is measured in terms of the specific area fall from in square centimetres per gram. The apparatus draws a definite volume of air through a prepared bed of cement. The porosity of the cement, which is a function of the size of the cement particles, determines the rate of air flow through the bed. The apparatus consists of a U-tube glass manometer, a ground joint with stainless steel test cell, a stop cock, and a rubber bulb.

3.4.2 Specifications of the Instrument

Table 2 Specifications of blaine apparatus

Disk	0.9 ±0.1 mm thick with 30-40 one mm diam. holes.
Cell.	Stainless steel; 12.70 ±0.10 mm
Plunger.	Stainless steel.
Manometer.	U-tube glass with ground joint, stop cock and rubber bulb assembly.
Filter Paper	12.70 mm diameter
Fluid.	Di butyl phthalate.
Weight.	Net 6 lbs. (2.8 kg).

3.5 Particle Size Analyser

Measuring and controlling the particle size distribution of cement is important both in order to achieve the desired product performance and to control manufacturing costs. Historic techniques of sieve and air permeability are still in use, but laser diffraction is becoming a more popular method to determine the particle size distribution of cement. The laser diffraction technique is quick, easy, reproducible, and provides a complete picture of the full size.

3.5.1 Measurement Techniques

Recently, modern cement laboratories deploy laser diffraction to perform particle size analysis. Laser diffraction trumps historic techniques with advantages in speed, ease of use, and reproducibility. In addition, laser diffraction provides a more complete description of the particle

size distribution. Although it is possible to correlate laser diffraction results to sieve and Blaine values, the correlation typically falls apart if the size distribution changes - a likely occurrence in a plant upset condition. Vendors of laser diffraction analyzers therefore promote the use of directly-calculated volume distribution results in the instrument's software package.

3.5.2 Experimental

Accurate measurement of cement in laser diffraction particle size analyzers proceeds either as a dry powder dispersed in air, or as a suspension dispersed in alcohol (isopropanol). We use here in this experiment the isopropanol because it does not react with cement.

3.5.3 Measuring Particle Size Using Laser Diffraction

The experimental set up of particle size analyser is shown in figure 7. Owing to the hard, robust nature of the material, all measurements are done in highest air pressure setting for the Powder Jet Dry Feeder. The Powder Jet maintains a constant mass flow rate through the measurement zone via clever use of an automatic feedback loop: control of vibration rate based on light source transmittance readings.

The system settings used for the dry measurements are presented below:

- Powder Jet: Small nozzle, max pressure
- Iteration number: 15
- Refractive index: 1.70-1.0 in 1.000 (air)



Figure 7 particle size analyser

3.5.4 Measurements Using Two Laser Diffraction Particle Size Analyzers

The wet results presented here were collected on both the LA-950 and LA-300 laser diffraction particle size analyzers. The LA-950 has a broader dynamic range (0.01-3000 μm) as compared to the LA-300 (0.1-600 μm), since the particle size of the cement is greater than 0.1 micron. Cement samples contain little to no powder below 0.1 μm , so both systems accurately and precisely measure the particle size of the cement. Note that all measurements were made in isopropanol (IPA). Monitoring the optical background is important when using IPA as thermal fluctuations may cause additional scattering leading to inconsistent results. When encountering this phenomenon, recirculating the IPA to obtain a stable background is typically required.

The system settings used for the wet LA-950 and LA-300 measurements are presented below:

- Iteration number: 15
- Refractive index: 1.70-1.0 in 1.390 (IPA)
- Ultrasound: 60s @ level 7 (full power)
- Circulation speed: 6
- Measurement time: 5000 acquisitions/second

3.6 Ball Milling

A ball mill is a type of grinder used to grind materials into extremely fine powder for use in paints, pyrotechnics, and ceramics. Ball mills rotate around a horizontal axis, partially filled with the material to be ground plus the grinding medium. Different materials are used as media, including ceramic balls, flint pebbles and stainless steel balls. An internal cascading effect reduces the material to a fine powder. Industrial ball mills can operate continuously, fed at one end and discharged at the other end. Large to medium-sized ball mills are mechanically rotated on their axis, but small ones normally consist of a cylindrical capped container that sits on two drive shafts (pulleys and belts are used to transmit rotary motion). A rock tumbler functions on the same principle. Ball mills are also used in pyrotechnics and the manufacture of black powder, but cannot be used in the preparation of some pyrotechnic mixtures such as flash powder because of their sensitivity to impact. High-quality ball mills are potentially expensive and can grind

mixture particles to as small as 0.0001 mm, enormously increasing surface area and reaction rates works on principle of critical speed.

3.6.1 Grinding Media



Figure 8 Grinding media with cement powder

There are many types of grinding media suitable for use in a ball mill, each material having its own specific properties and advantages. Common in some applications are stainless steel balls. While usually very effective due to their high density and low contamination of the material being processed, stainless steel balls are unsuitable for some applications, including:

- Black powder and other flammable materials require non-sparking lead, antimony, brass, or bronze grinding media
- Contamination by iron of sensitive substances such as ceramic raw materials. In this application ceramic or flint grinding media is used. Ceramic media are also very resistant to corrosive materials.

3.7 Compressive Strength Machine

This is the machine by which we can calculate the compressive strength of concrete sample up to 2000kN. This test is used to determine whether cement meets the compressive strength requirements of international standards. The test consists of casting a number of standard cubic specimens in laboratory conditions, using standard sands and then testing them for compressive strength after the required curing period has elapsed, normally 28 days. But in case of present work, the curing period was extended up to 90 days. The schematic view of the compressive strength machine is shown in figure 9.



Figure 9 compressive strength machine

CHAPTER-4

RESULTS AND DISCUSSION

4.1 X-Ray Fluorescence

X-ray fluorescence (XRF) is used to measure the chemical composition of samples. The XRF is done only some selected samples and value are given in table 3. The selections of the sample for the XRF are made on random basis.

Table 3 Chemical composition of the sample determined from XRF

Sample No.	SiO ₂	Al ₂ O ₃	Fe ₂ O ₃	CaO	MgO	P ₂ O ₅	Na ₂ O	K ₂ O	SO ₃	Cl	Total
PPC3	31.76	11.39	3.69	44.66	1.37	0.28	0.13	1.25	2.04	0.007	96.58
PPC5	31.39	10.91	3.61	44.68	1.38	0.26	0.14	1.25	2.06	0.009	95.69
PPC7	31.50	10.20	3.65	44.67	1.37	0.27	0.13	1.26	2.05	0.008	95.10

4.2 Important Factors and Chemical Analysis

There are some factors which are very important to estimate the compressive strength of the cement. These factors are derived from the chemical analysis of the sample. The factors are given below.

4.2.1 Lime Saturation Factor (LSF)

The LSF is a ratio of CaO to the other three main oxides. It is calculated as:

$$\text{LSF} = \frac{\text{CaO}}{(2.8\text{SiO}_2 + 1.2\text{Al}_2\text{O}_3 + 0.65\text{Fe}_2\text{O}_3)} \quad (7)$$

The LSF controls the ratio of tricalcium silicate (alite) to dicalcium silicate (belite) in the clinker. A clinker with a higher LSF will have a higher proportion of alite to belite. Typical LSF values in modern clinkers are lying between 0.92-0.98. At LSF=1.0 all the free lime might be combined with belite to form alite. If the LSF is higher than 1.0, the surplus free lime will remain as free lime. In practice, the mixing of raw materials is never perfect and there are always some regions within the clinker where the LSF is greater than 1 or less than 1. This means that there is almost

always some residual free lime, even where the LSF is considerably below 1.0. It also means that to convert virtually all the belite to alite, an LSF slightly above 1.0 is needed.

4.2.2. Silica Ratio (SR)

The silica ratio some times called “silica modulus” is defined as $SR = SiO_2 / (Al_2O_3 + Fe_2O_3)$. A high silica ratio means that more calcium silicates are present in the clinker on the cost of aluminate and ferrite. SR is typically between 2.0 and 3.0. The value of SR is 2.13 and is given in equation 8.

$$SR = SiO_2 / (Al_2O_3 + Fe_2O_3) = 2.13 \quad (8)$$

4.2.3. Alumina Ratio (AR)

The alumina ratio is defined as $AR = (Al_2O_3 / Fe_2O_3)$. This determines the potential relative proportions of aluminate and ferrite phase in the clinker. An increase in clinker AR (also sometimes written as A/F) means there will be proportionally more aluminate and less ferrite in the clinker. In Ordinary Portland Cement clinker, the AR is usually between 1 and 4 and in our composition this value is coming out to be 3.05 and represented in equation 9.

$$AR = (Al_2O_3 / Fe_2O_3) = 3.05 \quad (9)$$

4.3 Clinker: The Bogue Calculation

The standard Bogue [25] calculation refers to cement clinker, rather than cement, although it can be adjusted for use with cement. This is a very commonly-used calculation in the cement industry. The calculation assumes that the four main clinker minerals are pure minerals with their compositions. These four minerals are as follow:

Alite: C_3S or tricalcium silicate

Belite: C_2S or dicalcium silicate

Aluminate phase: C_3A or tricalcium aluminate

Ferrite phase: C_4AF or tetracalcium aluminoferrite

The above mentioned factors and compositions are responsible to decide the quality of the cement.

4.4 Particle Size Analysis

Particle size of the cement plays very important role to calculate the mechanical properties of the cement. Seven samples are selected and these samples are ball milled for different time durations. The particle sizes of these samples are measured with particle size analyser along with volume percentage. Additionally the blaine value concentration and specific surface area are also calculated for each sample. The typical plots of samples along with their respective particle size and volume percentage are given in figures (10-16). The data obtained from particle size analyser are summarized in table 4.

Table 4 Surface area with mean diameter and milling time

Sample Name	Ball milling (Minute)	Specific Surface Area (meter ² /gram)	Mean Diameter (μm)
PPC 1	0	.5799	32.62
PPC 2	30	.6072	29.92
PPC 3	45	.6384	27.77
PPC 4	60	.6874	28.01
PPC 5	80	.7329	25.69
PPC 6	95	.7748	26.80
PPC 7	120	.8468	22.96

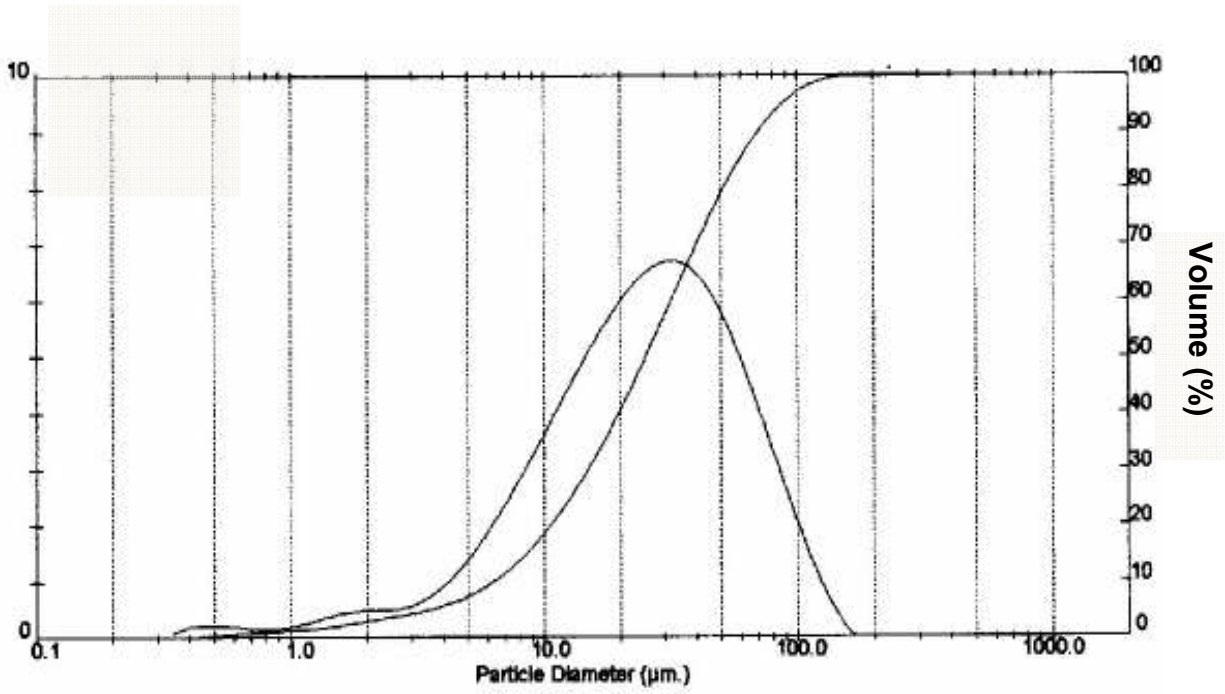


Figure 10 Particle diameter with respect to volume % of sample PPC1

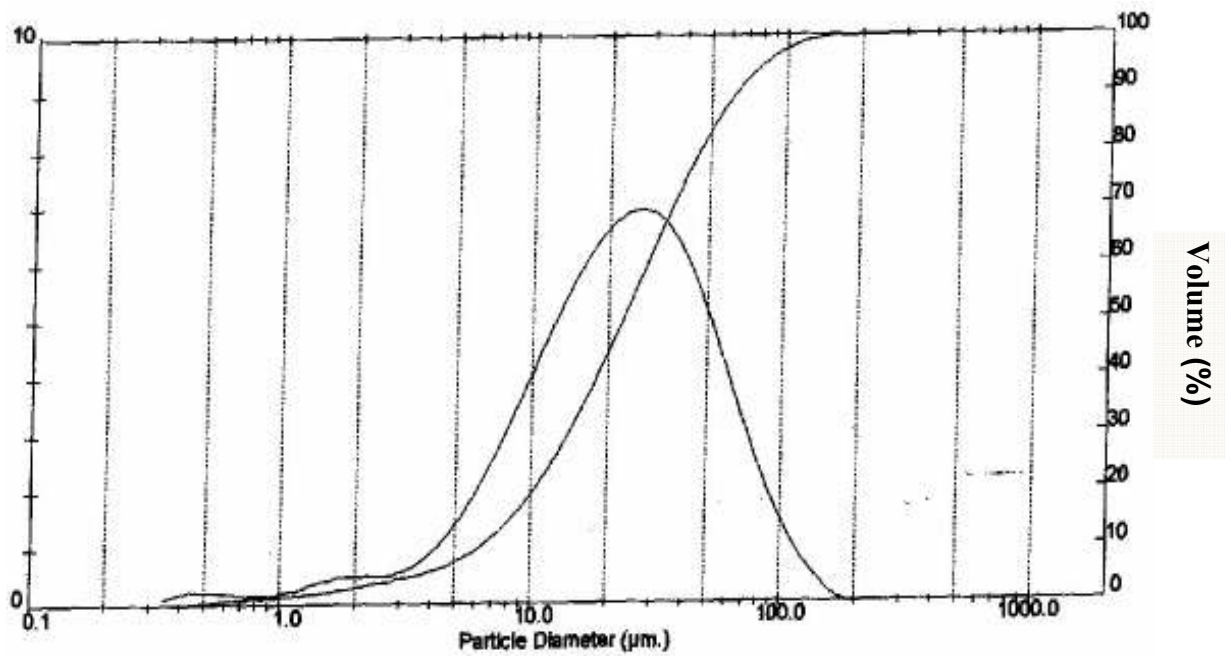


Figure 11 Particle diameter with respect to volume % of sample PPC2

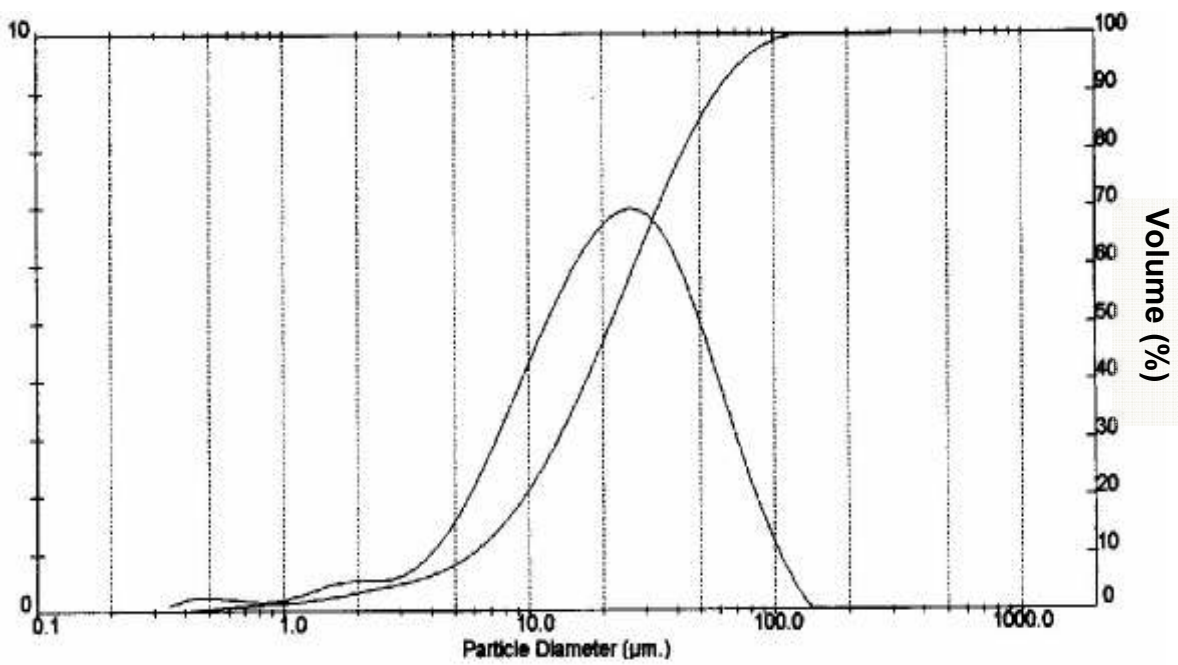


Figure 12 Particle diameter with respect to volume % of sample PPC3

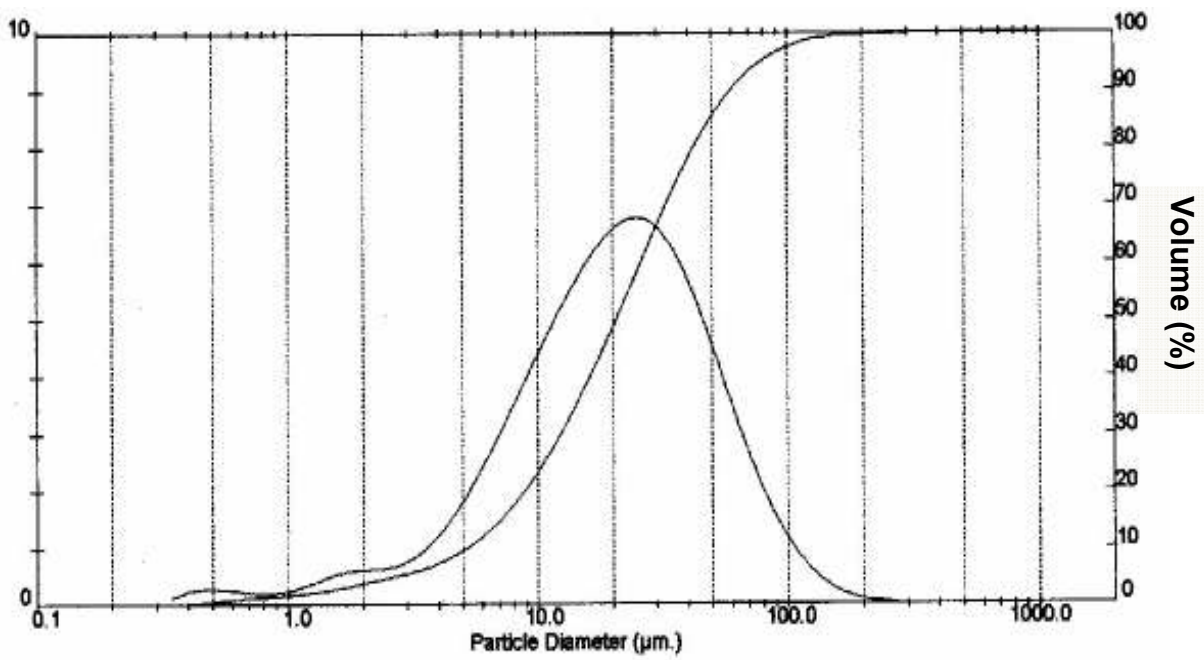


Figure 13 Particle diameter with respect to volume % of sample PPC4

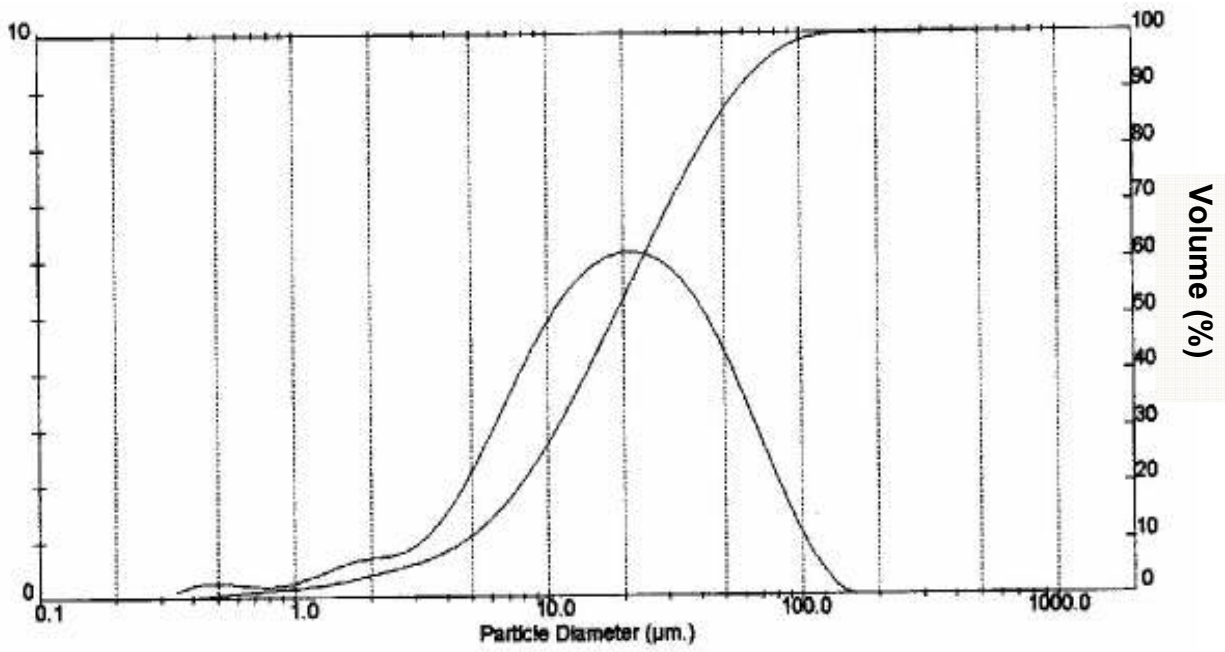


Figure 14 Particle diameter with respect to volume % of sample PPC5

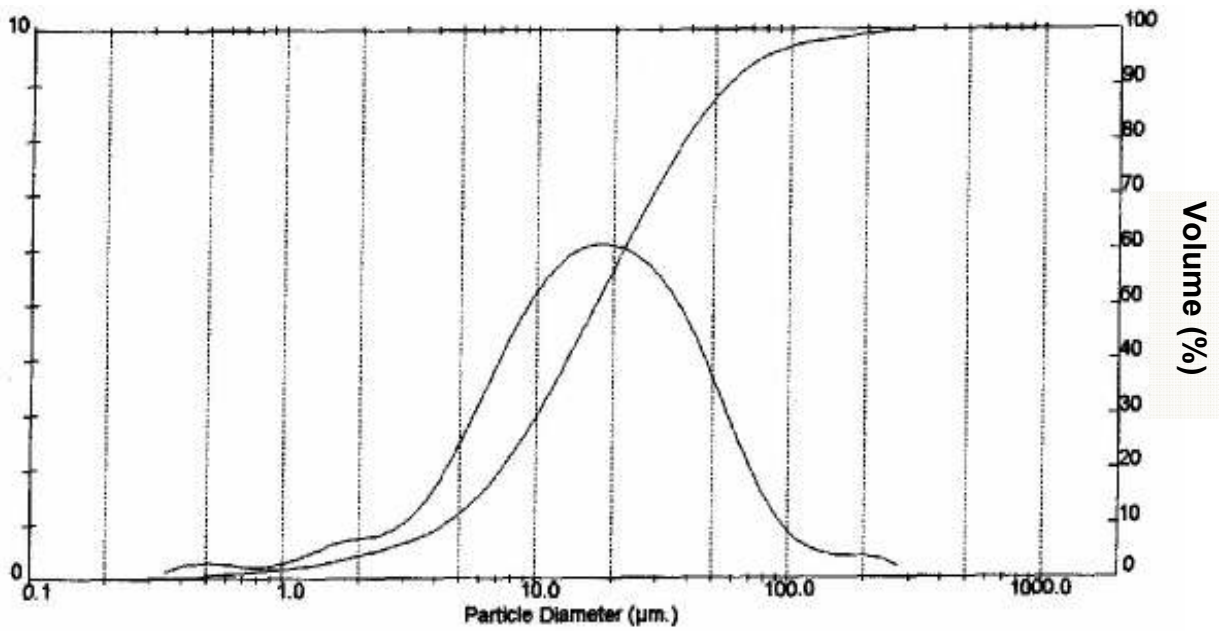


Figure 15 Particle diameter with respect to volume % of sample PPC6

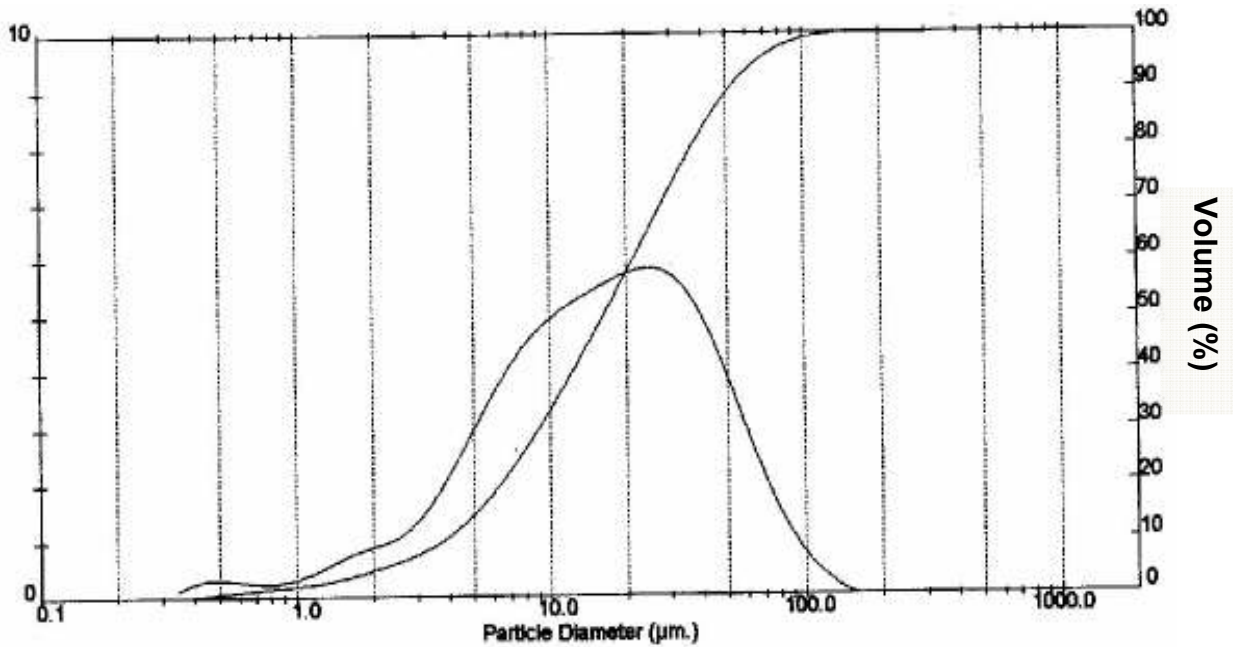


Figure 16 Particle diameter with respect to volume % of sample PPC7

The figures 10-16 clearly indicate that when we increase the milling time, correspondingly particle size is decreases in all the samples. On the other hand, their specific surface area increases with increases the ball milling time. These plots shows that the mean particle size of all the samples lying between 22-35µm.

4.5 X Ray Diffraction (XRD)

The XRD patterns of PPC3, PPC5, PPC7 samples are given in the figure 17. The XRD pattern of these samples could not show any appreciable difference in their pattern except some peaks broadening. According to the particle size analysis measurement, the mean particle size of the samples PPC3, PPC5, PPC7 are 28µm, 26µm and 22µm respectively. These samples exhibit CaO, SiO₂, Al₂O₃ and Fe₂O₃ as a major phases as mentioned in table 3 Basically the mean particle size of the samples varying only from 22-28µm, therefore, the particle size is calculated with the help of particle size analyser and XRD pattern could not resemble. This could be possible due to overlapping of the XRD peaks which belongs to various phases.

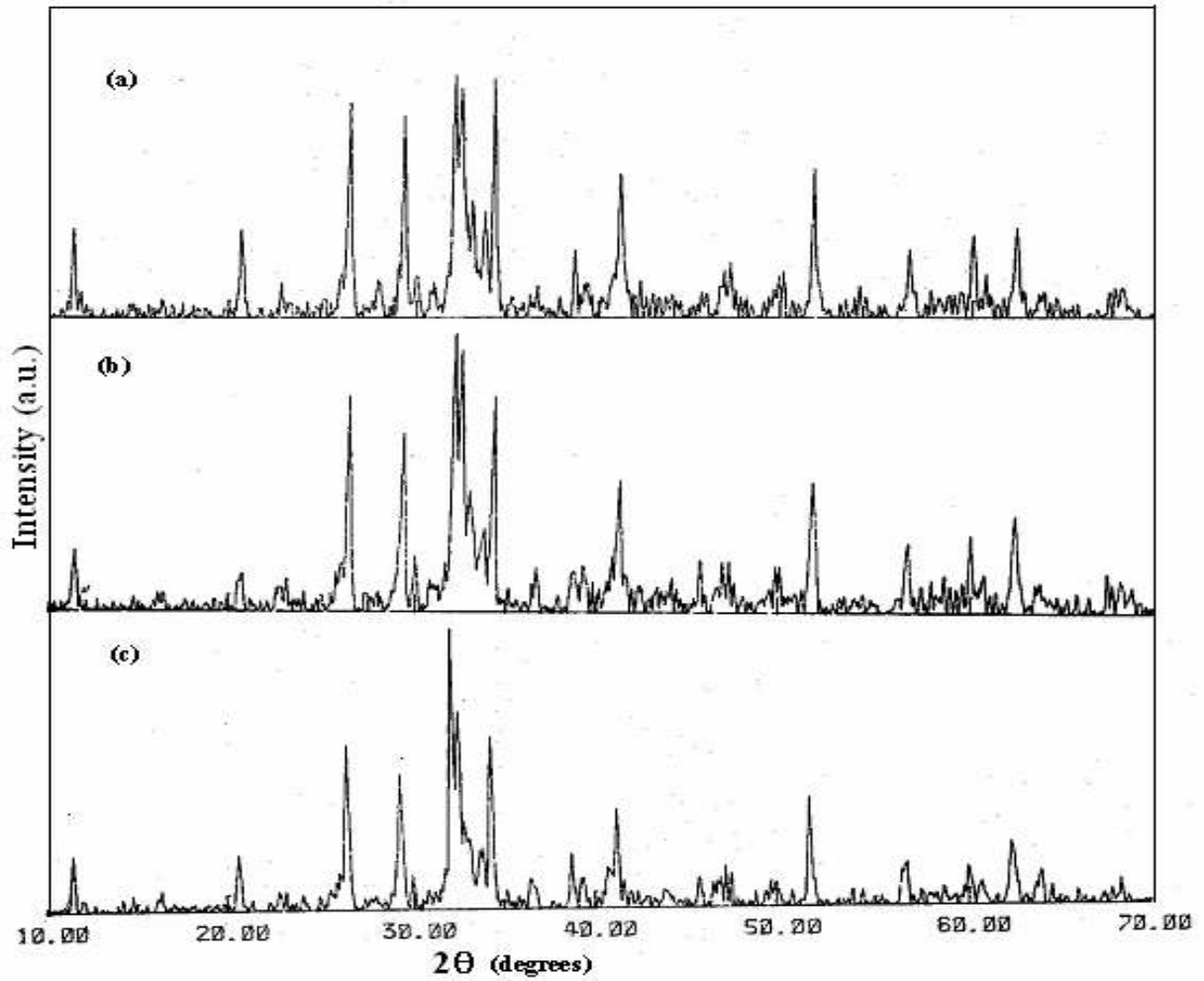


Figure17 The XRD pattern of the samples (a) PPC3 (b) PPC5 (c) PPC7

4.6 Compressive Strength Measurements

The compressive strength of all seven samples are measured using compressive strength machine. The compressive strength data were taken when it become constant respect to the applied load. The compressive strength versus curing time is given in table 5.

Table 5 Variation of compressive strength of various samples with days

Curing(Days)	Compressive strength (KN)						
	PPC1	PPC2	PPC3	PPC4	PPC5	PPC6	PPC7
1	163	172	178	180	183	187	189
3	316	323	329	331	336	337	342
7	400	417	430	432	450	458	466
28	585	590	597	601	612	622	628
60	684	703	710	714	716	719	727

Initially the strength of the sample increases rapidly with respect to the curing time. As the curing time increases the change in strength become less pronounced. The compressive strength of all the samples (table 5) increases as the size of cement particle decreases as shown in figure 18 and 19. While the smaller particle size rendered a larger specific surface area and high pozzolonic activity were produced. As a result, the cement with larger specific surface area showed a better performance in compressive strength. Similar results were reported by other researchers [55].

The plot of mean particle size (μm) versus compressive strength is plotted for different samples. The mean particle size of PPC 7 sample was found to be minimum as compared to other samples. This sample was ball milled for longer duration (2 hours). The minimum particle size sample exhibits the higher compressive strength of the specimen. However PPC1 sample shows lower strength as mean particle size of this sample is $32.8\mu\text{m}$. The compressive strength of the samples increases with increasing the curing time as shown in figure 18. In the figure anomaly was observed when the mean particle size varies between 26-28 μm . this implies that the compressive strength influence not only particle size but also proper distribution of particles (figure 11)

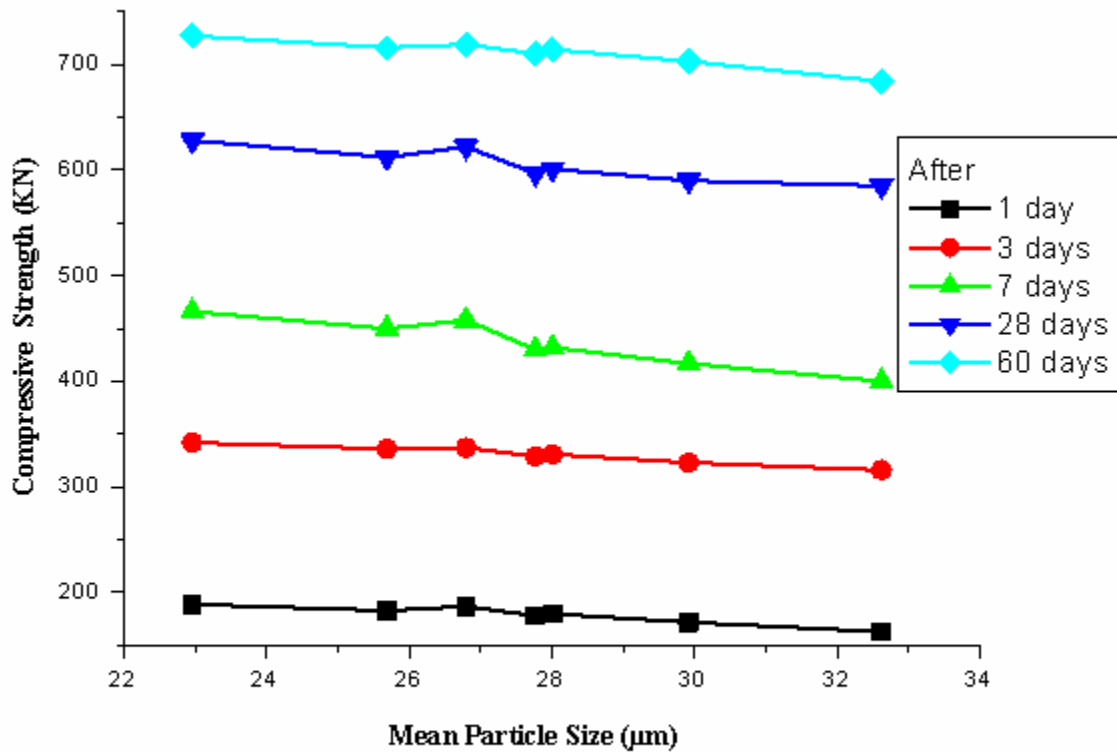


Figure18 Graph between compressive strength and mean particle size

The data obtained by the compressive strength measurement as shown in table 5 confirm that as we increases the milling time, there is decreases in particle size and correspondingly its strength is increasing.e.g.The strength of the sample PPC1 with particle size 32.62 µm is much lower then that of the sample PPC7 which has the mean particle size of 22.96 µm.

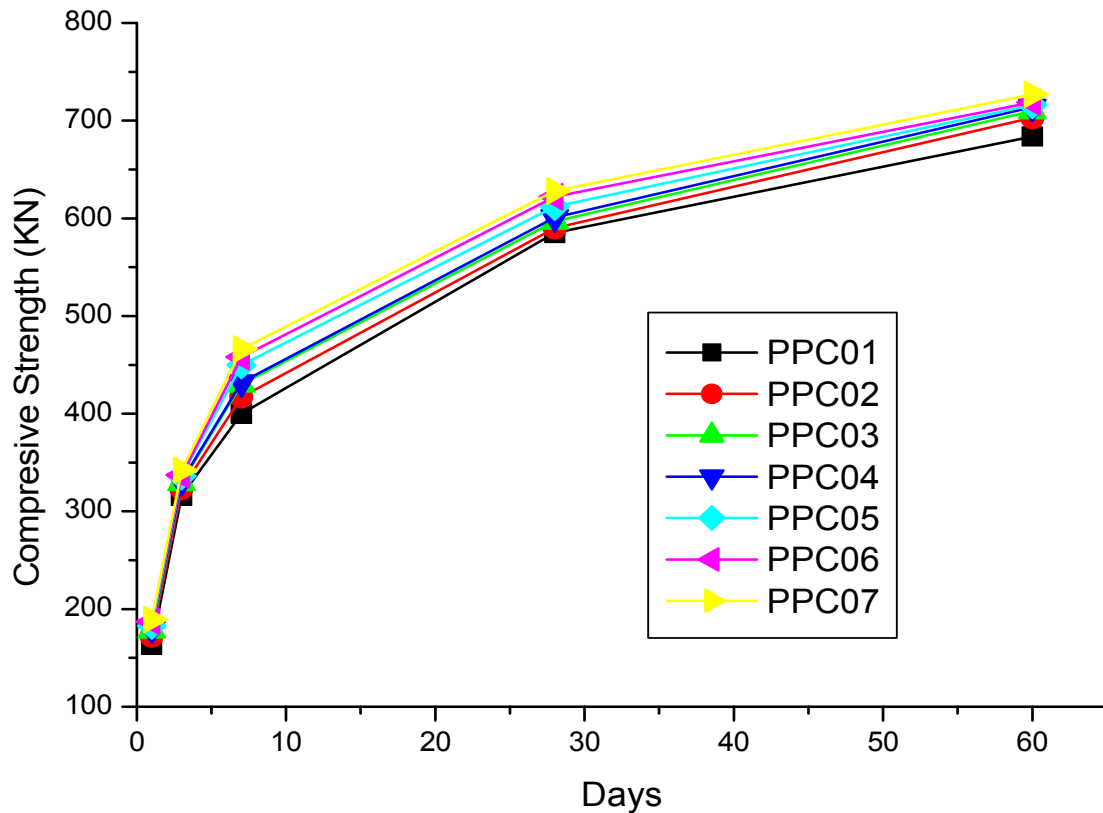


Figure 19 Graph between compressive strength and days

In the present samples, a finer material is likely to react more quickly than a coarser material. Differences in cement particle size, expressed as fineness or surface area, will affect the strength of the sample. The fineness to which the cement is ground will evidently affect the rate at which concrete strengths increase after mixing. Grinding the cement more finely will result in a more rapid increase in strength [16]. Fineness is often expressed in terms of total particle surface area of the sample, apart from this, particle size distribution is also very important therefore relying simply on surface area measurements can be misleading. Some minerals, for example gypsum can sometimes grind preferentially producing cement with a high surface area, with very fine gypsum and coarse clinker particles. Thus sample takes more time for setting with reduced compressive strength. Therefore, particle size as well as its proper distribution plays very important role to increases the strength of the cement. It also reduces the setting time of the cement. [10, 15]

CHAPTER-5

CONCLUSION AND FUTURE SCOPE

Seven samples are selected for the present study. These samples were grind ball mill for different time duration. These samples are analysed using particle size analyser, X ray fluorescence, X ray diffraction and compressive strength measurement. The chemical composition of the samples could not change after ball milling. The mean particle sizes of the samples varying from 22 μm to 33 μm . The sample PPC7 gives better results i.e. high compressive strength (727KN) because of its lower particle size then other samples. The compressive strength of the samples depends not only on particle size but also their distribution. Sample with larger specific surface area showed better performance with reducing setting time.

A better fineness and narrower particle size distribution can be obtained to change the ball mill parameters such as ball to cement ratio, speed and ball diameter etc. means grinding process. These parameters can be optimized after more experimentation with initial ingredients of the cement. The better particle size distribution also decreases the energy consumption during the heat of hydration. This can be achieved by optimized the various parameters during processing.

REFERENCES:-

1. W. Czernin: Zement-Kalk-Gips , 160 (1954)
2. F.Skvra, K.Kolp, J.Novotn, Z.Zadk: Cem.Concr.Res. i0, 253(1980)
3. H. Ritzman, Zement-Kalk-Gips 19, 390 (1968)
4. A.V.Vorovej and others: Proo. Moscow Cement Congress 1974, Vol. 3, p.21
5. F.kv-4ra, J.Konta: Silikty 22, 61 (1978)
6. EC. Higginson The effect of cement fineness on concrete. In: GJ Verbeck, editor. Fineness of cement. Philadelphia, PA: ASTM STP 473. American Society for Testing and Materials; 1970 (71–81).
7. B. Osbaeck, V.Johansen Particle size distribution and rate of strength development of Portland cement. J Am Ceram Soc 1989; 72:197–201.
8. G. Blunk, J. Brand, H. Kollo, U. Ludwing, Effect of particle size distribution of granulated blast furnace slag and clinker on the properties of blast furnace cements, Zement Kalk Gips (English Version) 2 (1989) 41–44.
9. S. Lee, H. Kim, E. Sakai, M. Daimon, The effect of particle size distribution of fly ash cement system on the fluidity of cement pastes, Cem. Concr. Res. 33 (2003) 763–768.
10. P.Dale Bentz,J.Edward Garboczi,J.Claus Haecker,M.Ole Jensen.Effect of particle size distribution on performance properties of portland cement-based materials.Cement and concrete research 29(1999) 1663-1671
11. K. Djamarani, I. Clark, Characterization of particle size based on fine and coarse fractions, Powder Technol. 93 (1997) 101–108.

12. F.T. Olorunsogo, Particle size distribution of GBFS and blending characteristics of slag cement mortars, *Cem. Concr. Res.* 28 (6) (1998) 907–919.
13. S. Grzeszczyk, G. Lipowski, Effect of content and particle size distribution of high calcium fly ash on the rheological properties of cement pastes, *Cem. Concr. Res.* 27 (6) (1997) 907–916.
14. K. Erdogdu, M. Tokyay, P. Türker, Comparison of intergrinding and separate grinding for the production of natural pozzolan and GBFS incorporated blended cements, *Cem. Concr. Res.* 29 (1999) 743–746.
15. P.K. Mehta, *Concrete, Structure, Properties and Materials*, Prentice-Hall, New Jersey, 1986.
16. Hanifi Binici, Orhan Aksogan, H. Ismail. Cagatay, Mustafa Tokyay, Engin Emsen .The effect of particle size distribution on the properties of blended cements incorporating GGBFS and natural pozzolan (NP) *Powder Technology* 177 (2007) 140–147
17. L. Beixing, L. Wenguan, H. Zhen, Composite Portland cement with a larger amount of industrial wastes, *Cem. Concr. Res.* 32 (2002) 1341–1344.
18. E.Fernandez, FJ.Gil , MP.Ginebra, FCM.Driessens, JA.Planell ,SM.Best. Production and characterisation of new calcium phosphate bone cements in the $\text{CaHPO}_4\text{-a-Ca}_3(\text{PO}_4)_2$ system:pH, workability and setting times. *J Mater Sci Mater Med*1999;10:223–30.
19. M.P. Ginebra,E. Fernandez, MG.Boltong, FCM Driessens,J.Ginebra, EAP.De Maeyer, Verbeeck, JA.Planell. Setting reaction and hardening of an apatitic calcium phosphate cement.*J Dent Res* 1997;76:905–12.
20. T.C.Powers. Estructura física de la pasta de cemento Portland. In:HF.W.Taylor química de los cementos. Bilbao:Ediciones Urmo; 1967. p. 444–72.

21. N.Moayed.AI-khalaf and A.Hana.Yousifl. Compactibility of no-fines concrete. The international Journal of Cement Composites and Lightweight Concrete, Volume 8, Number 7 February 1986
22. Sections of this document were obtained from the Synthesis of Current and Projected Concrete Highway Technology, David Whiting, et al, SHRP-C-345, Strategic Highway Research Program, National Research Council.
23. ACI Committee 223. 1983. Standard practice for the use of shrinkage-compensating ACI 223-83. Detroit: American Concrete Institute.
24. ACI Committee 225R. 1985. Guide to the selection and use of hydraulic cements. AC225R-85. Detroit: American Concrete Institute.
25. R. H. Bogue 1955. The chemistry of portland cement. 2d ed. New York: Reinhold PublishingCorp.
26. B. M. Call, 1979. Slump loss with type "K" shrinkage compensating cement, concrete, and Admixtures. Concrete International: Design and Construction, January: 44-47.
27. Energetics, Incorporated. 1988. The U.S. cement industry: An energy perspective. Final report. Columbia, Md.: Energetics, Incorporated.
28. G. C. Hoff, 1985. Use of steel fiber reinforced concrete in bridge decks and pavements. In Steel fiber concrete seminar (June): Proceedings, ed. S. P. Shah and A. Skarendahl, 67-108. Elsevier Applied Science Publishers.
29. G. C. Hoff,L. N. Godwin, K. L. Saucier, A. D. Buck, T. B. Husbands, and K. Mather. 1977. Identification of candidate zero maintenance paving materials. 2 vols. Report no. FHWA-RD-77-110 (May). Vicksburg, Miss.: U.S. Army Engineer Waterways Experiment Station.

30. Kudlapur, P. A. Hanaor, P. N. Balaguru, and E. G. Nawy. 1987. Repair of bridge deck structures in cold weather. Report no. SNJ-DDT4-25156 (December). The State University of New Jersey, College of Engineering, Dept. of Civil Engineering.
31. D. Y. Lee, 1973. Review of aggregate blending techniques. Highway Research Record, no. 441 111-98
32. F. Massazza, 1987. The role of the additions to cement in the concrete durability. Cemento 84(October-December):359-82.
33. W. J McCarter, and S. Gravin. 1989. Admixture in cement: A study of dosage rates on early hydration. Materials and Structures 22:112-120.
34. P. K. Mehta, 1986. Concrete. Structure, properties, and materials. Englewood Cliffs, N.J. Prentice-Hall, Inc.
35. L. M. Meyer, and W. F. Perenchio. 1979. Theory of concrete slump loss as related to use of chemical admixtures. Concrete International. Design and Construction 1 (1):36-43.
36. R. Mielenz, 1984. History of chemical admixtures for concrete. Concrete International: Design and Construction 6 (4):40-54 (April).
37. Mindess, and J. F. Young. 1981. Concrete. Englewood Cliffs, N.J.: Prentice-Hall, Inc.
38. National Material Advisory Board. 1987. Concrete durability: A multi-billion dollar opportunity. NMAB-437. Washington: National Academy Press.
39. Polivka, and A. Klein. 1960. Effect of water-reducing admixtures and set-retarding admixtures as influenced by cement composition. In Symposium on effect of water reducing admixtures and set-retarding admixtures on properties of concrete. STP-266, 124-39. Philadelphia: American Society for Testing Materials

40. D. Pomeroy, 1989. Concrete durability: From basic research to practical reality. ACI special publication. Concrete durability SP- 100: 111-31.
41. N. J. Popoff, 1991. Blended cements. A vision for the nineties. Concrete technology seminar MSU-CTS no. 5 (February), eds. P. Soroushian and S. Ravanbakhsh, 2.1-2.16. East Lansing: Michigan State University.
42. Powers, T. C., L. E. Copeland, J. C. Hayes, and H. M. Mann. 1954. Permeability of portland cement paste. ACI Journal Proceedings 51 (3):285-98.
43. Previte, R. 1977. Concrete slump loss. ACI Journal Proceedings 74 (8):361-67.
44. Ramachandran, V. S., and R. F. Feldman. 1984. Cement science. In Concrete admixtures handbook: Properties, science, and technology, ed. V. Ramachandran, 1-54. Park Ridge, N.J. Noyes Publications.
45. Ruetters, A., E. N. Vidal, and S. P. Wing. 1935. An investigation of the permeability of mass concrete with particular reference to Boulder Dam. ACI Journal Proceedings 31:382-416.
46. Standard specification for portland cement (AASHTO M 85-89). 1986. AASHTO standard specification for transportation materials. Part I, Specifications. 14th ed.
47. Standard specification for portland cement (ASTM C 150-86). 1990 annual book of ASTM standards 4.02:89 - 93.
48. Taylor, W. F. W., ed. 1964. The chemistry of cements. 2 volumes. London: Academic Press.
49. Tsuji, and N. Miyake. 1988. Chemically prestressed precast concrete box culverts. Concrete International: Design and Construction 10 (5):76-82 (May).
50. U.S. Department of the Interior. Bureau of Mines. 1989. Cement mineral yearbook. Washington: GPO.

51. U.S. Department of Transportation. Federal Highway Administration. 1990. Portland cement concrete materials manual. Report no. FHWA-Ed-89-006 (August). Washington: FHWA.
52. G. J. Verbeck, 1968. Field and laboratory studies of the sulfate resistance of concrete. In Performance of concrete resistance of concrete to sulfate and other environmental conditions: Thorvaldson symposium, 113-24. Toronto: University of Toronto Press.
53. Whiting, 1981. Evaluation of super-water reducers for highway application. FHWA/RD 80/132 (March). Washington: FHWA.
54. P. Dale Bentz. Influence of cement particle size distribution on early age autogenous strain and stresses in cement based materials. NIST Gaithersburg, MD 20899-8621,
55. K.L. Lina, W.C. Chang, D.F. Linc, H.L. Luoc, M.C. Tsaic. Effects of nano-SiO₂ and different ash particle sizes on sludge ash-cement mortar Journal of Environmental Management Received 10 April 2006; received in revised form 8 March 2007; accepted 25 March 2007